Computational Materials Science 71 (2013) 192–196

Contents lists available at SciVerse ScienceDirect

Computational Materials Science

journal homepage: www.elsevier.com/locate/commatsci

Ab initio study of CO adsorption on PdGa(1 1 0)

P. Bechthold, P.V. Jasen, J.S. Ardenghi, E.A. González, A. Juan *

Departamento de Física & IFISUR (UNS-CONICET) – Universidad Nacional del Sur, Av. Alem 1253, 8000 Bahía Blanca, Argentina

ARTICLE INFO

Article history:
Received 21 September 2012
Received in revised form 23 January 2013
Accepted 24 January 2013

Keywords:
PdGa
DFT
Intermetallic compounds
CO adsorption

ABSTRACT

CO adsorption is analyzed using Density Functional Theory (DFT) calculations. Changes in the electronic structure of PdGa(1 1 0) surface and CO bond after adsorption are addressed. CO is located only on Pd atop geometry with a tilted configuration (9.13° from the perpendicular to the surface) and no interaction with Ga is detected. The Pd–Pd bond strength decreases 54.2% as the new Pd–CO bond is formed. The C–O bond length change less than 1%, compared to the gas phase value, while its bond overlap population decrease 46.2%. The effect of CO is limited to its first Pd neighbor. Analysis of orbital interaction reveals the Pd–CO bond mainly involves s–s and s–p orbitals with less participation of Pd 4d orbitals. The computed CO vibration frequencies after adsorption shows a red shift from vacuum to ward 2013.85 cm^{-1}, which agrees with previous experimental data on PdGa intermetallic.

1. Introduction

Energy carriers are used to store, move and deliver energy in an easily usable form. The conversion of energy to electricity makes easily its transportation. Hydrogen is one of the most promising energy carriers for the future. It is a high efficiency, low polluting fuel that can be used for transportation, heating, and power generation in places where it is difficult to use electricity [1].

Since hydrogen gas is not found free on Earth, it must be manufactured. There are four basic methods for hydrogen production at present: steam reforming reaction, partial oxidation, auto-thermal reforming and water electrolysis.

The most frequently used process in industry is the steam reforming of hydrocarbons or oxygenates. In the oxygenates category, the methanol is particularly important for industrial process, because is easy to handle and store.

Methanol steam reforming (MSR, $CH_3OH + H_2O \rightarrow 3H_2 + CO_2$) is considered as one of the most promising routes to produce high purity hydrogen for mobile fuel cell applications. However, the main drawback is the formation of CO as a byproduct, which has to be kept at a level of less than 20 ppm to prevent poisoning of fuel cell catalysts.

In 1993, Iwasa et al. reported [2] that Pd/ZnO is a highly selective catalyst for steam reforming of methanol. Since then, several Pd-based catalysts have been studied [3–7] in search of possible alternatives for use in efficient hydrogen production.

Recently Rameshan et al. [8] made a XPS study of methanol reforming on the intermetallic compound PdGa. They report that PdGa is a poor unselective catalyst in MSR, but it is highly CO_2 selective and active in presence of O_2. So this unsupported catalyst could be use in an oxidative methanol steam reforming process (OMSR, $CH_3OH + 1/2O_2 \rightarrow 2H_2 + CO_2$) to obtain hydrogen. The advantage of using an unsupported catalyst, instead of the commonly used supported catalyst, is that the composition of the catalyst surface is well defined; present more structural stability, and less deactivation.

The concept of using intermetallic compounds with covalent bonding rather than alloys is a suitable way to arrive at long-term stable catalysts with pre-selected electronic and local structural properties [9–13]. An "intermetallic compound" is a chemical compound of two or more metallic elements and adopts an at least partly ordered crystal structure that differs from those of the constituent metals [14].

The study of CO adsorption on Pd–Ga systems is rather scarce [1,8,9,15].

With the aim of contribute to the understanding of the interactions between the CO (also an OMSR byproduct) and the intermetallic PdGa compound as catalyst, computational DFT calculations are performed to determine the binding energies of CO and the changes in the intermetallic PdGa compound surface, after the CO adsorption.

2. Surface models and computational method

The PdGa intermetallic compound presents a $P2_13$ structure with a lattice parameter of $a_0 = 4.909$ Å (see Fig. 1a) [16–18]. A refined crystal structure of (1:1) PdGa was recently reported [19]. This intermetallic compound has a simple cubic distortion, where seven Ga atoms surround each Pd. We selected the (1 1 0)

* Corresponding author. Tel.: +54 291 4595101x2818; fax: +54 0291 4595142.
E-mail address: cajuan@uns.edu.ar (A. Juan).

0927-0256/$ - see front matter © 2013 Elsevier B.V. All rights reserved.
http://dx.doi.org/10.1016/j.commatsci.2013.01.033

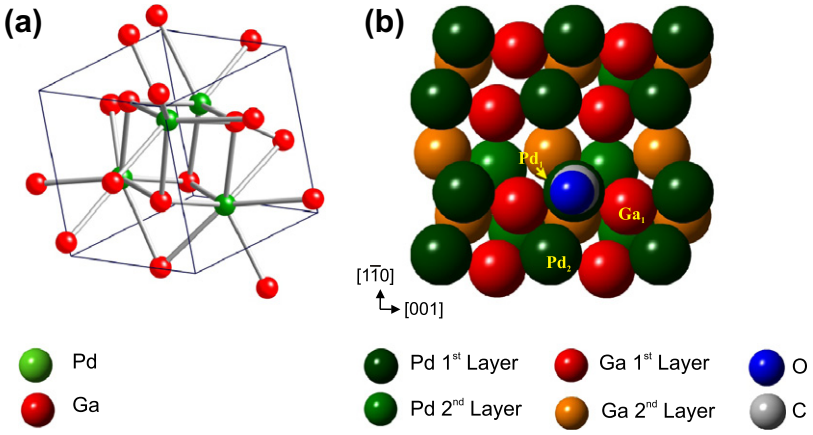

Fig. 1. Crystal structure for PdGa (a). Schematic top view of PdGa(1 1 0) surface after CO adsorption. For sake of clarity, only two first layers are shown.

crystallographic plane because it is the cleavage plane, and as low index plane it could be exposed as a catalytic surface. Experimental studies of Verbeek et al. conclude that this plane shows no reconstruction [19]. Density Functional Theory (DFT) is used to compute adsorption energies, trace relevant orbital interactions, and discuss the electronic consequences of incorporating CO to the surface. In the next sections we will consider, the computational method and adsorption models.

2.1. Computational method

We performed first-principles calculations based on spin polarized DFT. The Vienna *Ab initio* Simulation Package (VASP) is used to solve Kohn–Sham equations with periodic boundary conditions and a plane wave basis set [21–23]. Electron-ion interactions were described by ultra-soft pseudopotentials [24], exchange and correlation energies were also calculated using the Revised Perdew–Burke–Ernzerhof form of the spin-polarized generalized gradient approximation (GGA-RPBE), which has been shown to give accurate values for adsorption energies of many molecular species [25]. We used a kinetic energy cutoff of 290 eV for all calculations, which converges total energy to ~1 meV/atom and 0.001 Å for the primitive bulk cell. The Monkhorst–Pack scheme is used for k-point sampling [26]. An equilibrium lattice constant of 4.899 Å is used as obtained with a $7 \times 7 \times 7$ converged mesh within the first Brillouin Zone. The geometry optimization was terminated when the Hellman–Feyman force on each atom was less than 0.02 ev/Å and the energy difference was lower than 10^{-4} eV. The lattice constant is in agreement with experimental XRD data. Bader analysis is used to calculate electronic charges on atoms before and after CO adsorption [27]. The adsorption energy is calculated using following equation:

$$\Delta E_{ads} = E_{Total}(CO/PdGa) - E_{Total}(PdGa) - E_{Total}(CO) \quad (1)$$

Here the first term on the right-hand side is the total energy of the super cell that includes 32 Pd and 32 Ga atoms and one CO molecule; the second term is the total energy of the intermetallic super-cell; the third term is the CO molecule total energy. The last one is calculated by placing CO in a cubic box with 10 Å sides and carrying out a Γ-point calculation. We obtained a CO bond length of 1.143 Å in fairly good agreement with experimental values [28].

In order to understand CO–PdGa interactions and bonding we used the concept of Density of States (DOS) and the Crystal Orbital Overlap Population (COOP) as described by Hoffmann [29]. The COOP curve is a plot of the OP weighted DOS vs. energy. Looking at the COOP, we analyzed the extent to which specific states contribute to a bond between atoms or orbitals [29]. The SIESTA code was used to compute COOPs [30,31].

2.2. Surfaces and adsorption model

We represented the (1 1 0) plane with a super-cell. In order to achieve the best compromise between computational time and accuracy of our model, we decided to use a seven-layer slab separated in the [1 1 0]-direction by vacuum regions. It should be pointed out that each "layer" is formed by three "sub-layers", presenting atoms above and below. We also tested our calculations with 9 and 11 layers (and the corresponding sub layers) and no further improvement in energy was found. The thickness of the vacuum region, corresponding to 10 Å, was enough in order to avoid the interaction of CO molecule on the surfaces. The thickness of the PdGa(1 1 0) slab should be such that it approximates the electronic structure of 3D bulk PdGa in the innermost layer. The interlayer spacing in this PdGa(1 1 0) model is 1.745 Å. This value is not the common interplanar distance of a simple cubic structure, because every plane has atoms below, in, and above the middle line. This means that each line has three different values in the [1 1 0] direction. The (1 1 0) plane presents two possible terminated surfaces, Pd or Ga, but we analyzed only the former because it has better catalytic properties and Ga terminated surface does not adsorb CO [9]. Recent calculations from our group support this finding of non-active Ga as chemisorption sites [32].

For the study of CO adsorption on the PdGa(1 1 0) surface at low coverage, the CO-surface distance was optimized considering relaxation for the first four layers of the metal slab until 1 meV convergence was obtained in the total energy, maintaining the three remaining layers fixed (bulk like). Due to the Pd coordination in the bulk structure, almost any exposed plane present isolated Pd sites, being the next neighbor Pd located at a mean distance of 4 Å or more. This fact does not allow us to make any conclusion about the effect of CO coverage because the CO–CO interaction at this distance was very weak. Figs. 1b and 2 show a schematic top and side view of the surface after CO adsorption, respectively.

3. Results and discussion

We reported in a previous study a very good agreement between the experimental data and the computed bulk modulus, equilibrium lattice constant and electronic structure (DOS) for PdGa bulk [9,16–20,32]. Our DOS calculation completely agrees with that of Kovnir et al. [9,14]. We also compared the computed

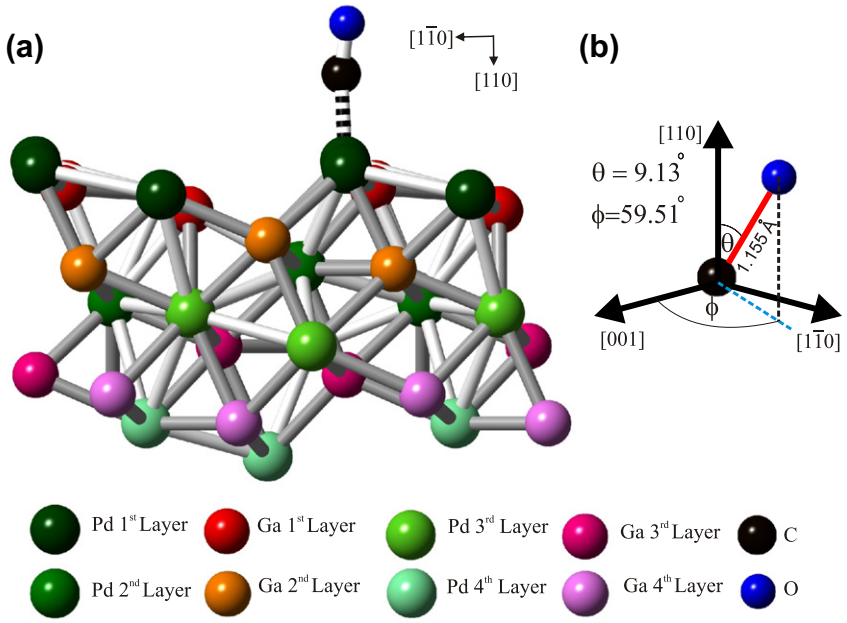

Fig. 2. Schematic lateral view of PdGa(1 1 0) surface after CO adsorption (a) and geometrical view of CO molecule adsorbed (b).

PdGa covalent bonding scheme on the (1 1 0) surface with recent NMR results of Klanjek et al. [12].

We found CO on the top Pd site (see Fig. 2) at a Pd–CO distance of 1.996 Å and stabilization energy of −1.42 eV. Considering the CO adsorption on top on pure FCC Pd surface, Chen et al. reported −1.17 eV for the (1 1 1) plane while Pick found a corrected value of −1.19 eV in the (1 1 0) surface [33,34]. The last author also reports a Pd–CO distance of 1.91 Å. In the case of a Pd nano-clusters with a hybrid 5-fold-symmetry/close-packed structure Paz-Borbon et al. obtained an adsorption energy of −1.42 eV for a CO bonded in a top position [35].

When adsorbed, the C–O distance does not change significantly compared with the molecule in vacuum (see Table 1). Our computed C–O distance in vacuum is 1.143 Å, which is close to 1.131 Å determinate from XRD data [28]. A similar C–O distance is also reported by pick for CO/Pd(1 1 0)(1.168 Å) [34]. It should be mentioned that this author reports a perpendicular on-top geometry. We found a 9.13° tilted configuration (see Fig. 2). From the analysis of IR data, Kovnir et al. [9] assigned an on top position for CO on PdGa compound.

Table 1
Electron orbital occupation, overlap population (OP), ΔOP% and distances for PdGa and CO/PdGa.

Structure	Electronic occupation			Bond type	OP	ΔOP%	Distances (Å)
	s	p	d				
PdGa							
Pd	0.80	0.22	9.88	Pd_1–Pd_2	0.142		3.016
Ga	1.71	0.44	0.00	Pd_1–Ga_1	0.137		2.710
CO (vacuum)							
C	0.44	0.38	0.00	C–O	0.854		1.143
O	1.61	3.56	0.00				
CO/PdGa							
Pd	0.57	0.73	9.64	Pd_1–Pd_2	0.065	−54.2	3.094
Ga	1.72	0.27	0.00	Pd_1–Ga_1	0.133	−2.9	2.593
C	1.12	4.26	0.00	Pd_1–C	0.921		1.967
O	1.62	5.84	0.00	C–O	0.459	−46.2	1.155

As mentioned before, the PdGa intermetallic compound [16–18] has each Pd surrounded by seven Ga atoms. When the (1 1 0) plane is generated from the bulk, an isolated Pd atom is exposed. Therefore, a comparison with PdCO molecule and Pd_nCO (n = 1–9) is relevant. The gas phase experimental study of this molecule found a linear geometry with a $^1\Sigma^+$ ground state and Pd–C and C–O distances of 1.845 Å and 1.137 Å, respectively [36]. The computed Pd–C and C–O bond strengths shows a noticeable degree of convergence of values in recent years [37]. DFT and all electron (CCSD(T)) calculation including relativistic effects agree with experimental data [37,38]. In the case of Pd_nCO clusters, the DFT study of Bertin et al. [39] predicted a linear geometry if n = 1 with the CO bond length (1.18 Å) not appreciably modified after the interaction with a single Pd atom. Schultz et al. presented similar results from *Ab initio* calculations for Pd_nCO (n = 1,2) [40]. Zanti and Peeters performed a DFT study of small Pd_n clusters (n = 1–9)–CO [41]. Their results (d_{Pd-C} = 1.867 and d_{C-O} = 1.138 Å) are close to our present calculations when n = 1. Kalita and Deca reported a Pd–CO distance and C–O bond length in neutral and charged Pd_1CO of 1.868 and 1.161 Å, respectively [42].

Considering the electronic structure, and as expected, we found no significant change in the Fermi level after CO adsorption (see Fig. 3 –DOS–). The total DOS is dominated by the many bulk-like and surface Pd and Ga atoms, so that the changes are subtle but visible in the Pd projected DOS. The plot in Fig. 3b shows a decrease in the Pd d bond density and a small shift of about 0.60 eV to lower energies. A similar behavior was computed for the DOS of Pd atoms bonded to CO on the (1 1 0) FCC naked surface [34]. In a theoretical study of CO adsorption on Pd(2 1 0) surface Lischka et al. [43] described the CO bonding to the metal surface in terms of the Blyholder model [44] and the analysis of the resulting mixed orbitals [45,46] upon CO adsorption, the Pd–d band center is shifted down 0.56 eV. XPS results of Kovnir et al. [9] indicate no change in the electronic structure of the PdGa intermetallic surface upon reaction conditions. These conclusions are in full agreement with our present results on the effect of CO on the electronic structure of PdGa (1 1 0) surface.

Almost no change in DOS is detected for Ga after CO adsorption (see Fig. 3c). Fig. 3a shows the total DOS of the system with CO contribution. The bands at ∼−5 and ∼−10 eV corresponds to

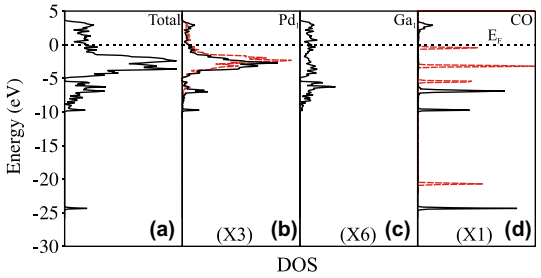

Fig. 3. Total DOS curves for CO/PdGa(1 1 0) (a); projected DOS for a Pd atom (b); projected DOS for a Ga atom (c) and projected DOS for a CO molecule (d). Before (red dashed line), after CO adsorption (black fill line). (For interpretation of the references to color in this figure legend, the reader is referred to the web version of this article.)

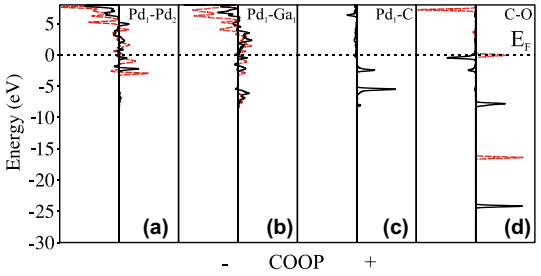

Fig. 4. Pd–Pd, Pd–Ga, Pd–C and C–O COOP curves for PdGa(1 1 0) surface before (red dashed line) and after (black filled line) CO adsorption (a–d).

contributions from CO orbitals interacting with Pd orbitals, which becomes stabilized after adsorption. This is clearly shown in Fig. 3d -compare solid (CO/PdGa) and doted lines (CO in vacuum). The peak at –24.2 eV in the total DOS correspond mainly to CO orbitals that almost do not interact with the surface (see Fig. 3b). This picture is similar to that computed by Lischka et al. [43]. It should be mentioned that projected DOS of CO shows very narrow bands, which is an indication of an interaction with an "isolated Pd site".

An analysis of the bonding between CO and the surface reveals that the main contribution to the Pd–CO bond comes from s–p (42.7%), s–s (23.6%) and p–p (31.0%) orbitals. Less than 2% of the bonding comes from p–d interactions (see Table 2). The Pd–CO bond is achieved at expense of weakening Pd_1–Pd_2 nearest neighbor (see Table 1 and Fig. 4a). Thus, the Pd_1–Pd_2 bond overlap population (OP) involving Pd atoms directly bonded to CO is reduced to 54.2% of its original value on the clean PdGa surface. The COOP curves in Fig. 4a also shows less bonding after CO adsorption. Paz-Borbon et al. [35] found an overall inflation of the Pd nano-clusters and a weakening of the metal-metal bonds. The Pd_1–Ga_1 OP presents a small change (2.9% in Table 1. Also see Fig. 4b). The Pd_1–Ga_1 sp contribution to the bonding decrease while the p–d contribution increase after CO adsorption (see Table 2). These are indications that surface nearest neighbors to Pd_1, (Pd_2 and Ga_1) are also involved in CO bonding, being these interactions the reason for the small CO tilting angle.

Regarding CO, its bond length is 4.5% shortened after adsorption. The C–O bond is weakened due to 5σ donation and $2\pi^*$ back donation to the surface. This is show in Table 1 where C 2p orbitals are more populated after CO adsorption being the more affected the p_x and p_y orbitals. The C–O OP decrease 46.2% while its bond length change less than 1.05%. The Pd d orbital population change $0.24e^-$, which is consistent with the main role of s–s and s–p interaction (see Table 1). The reasons of this C–O bond weakening are mentioned by Shultz et al. [40], Bertin et al. [39], Filatov et al. [37] and Zanti and Peeters [41]. According to these last authors, the intensity of back bonding results in the relocalization of $0.30e^-$ from the 4d orbitals of Pd [41] in good agreement with our results.

Finally, we also computed the stretching vibration frequencies for CO bonded to the surface. In order to do this, we used a whole vibrational mode with an important contributions for C–O bond. The experimental C–O frequency (gas phase) is 2170 cm^{-1} [47] while our computed value is close (2136.56 cm^{-1}) in good agreement with that reported by Lischka et al [43]. After adsorption, this vibration frequency is 2013.85 cm^{-1} while for Pd–C is 249.04 cm^{-1}. The computed red shift of the CO vibrating frequency is similar to that reported for the PdCO molecule and Pd_nCO clusters [37–42]. In the case of Pd–C frequency, our result is within the range 234.30–256.60 cm^{-1} reported in [38].

It is worth mentioning some literature results obtained from FT-IR studies. This is the case for CO adsorption on PdGa and Pd/Al_2O_3 samples [9]. The complete isolation of Pd on the PdGa surface shows a significant red shift of CO vibrational frequency to 2047 cm^{-1}. This band was assigned to CO adsorption on Pd in on-top position, being the red shift a result of negatively charged Pd [9]. Low temperature experiments revealed a fine structure of the adsorption bands and were attributed to at least three different isolated Pd atoms. These facts will be the aim for future theoretical calculations.

Table 2
Orbital by orbital percentage contributions to Pd_1–Pd_2, Pd_1–Ga_1, Pd_1–C, and C–O overlap populations (%COOP) for CO/PdGa(1 1 0) system.

	Pd_1–Pd_2		Pd_1–Ga_1		Pd_1–C	C–O	
	PdGa	CO/PdGa	PdGa	CO/PdGa	CO/PdGa	Vacuum	CO/PdGa
s–s	40.6	16.4	13.3	14.1	23.6	24.2	26.0
s–p	35.7	34.7	67.4	50.1	42.6	56.5	62.9
s–d	5.4	15.7	0.0	0.0	1.0	–	–
p–p	5.5	13.4	11.8	14.1	31.0	19.3	11.1
p–d	12.2	19.8	7.5	21.7	1.8	–	–
d–d	0.0	0.0	–	–	–	–	–

4. Conclusion

The adsorption of CO in $P2_13$ PdGa alloy has been studied by DFT calculation. The adsorption energy is −1.42 eV with respect to the gas phase CO molecule. This result is similar to those computed for CO on top sites on FCC Pd metallic surfaces and Pd nano-clusters. The CO distance do not change significantly with respect to the isolated molecule but its overlap population decrease 46.2% while a Pd–C bond is developed.

The CO adsorb atop on a Pd atom with a small tilt of 9.13°. And present an analogy with the PdCO molecule and Pd_nCO (n = 1,9) clusters.

The Pd–CO bond is formed at the expenses of Pd–Pd bonding and no interaction with Ga is detected. The main contribution to Pd–CO bonding corresponds to s–s and s–p orbitals with less participation of Pd 4d orbitals. A back donation of about $0.23e^-$ is also computed. Surface nearest neighbors to Pd_1, (Pd_2 and Ga_1) are also involved in the CO bonding, being this the reason for the small CO tilting angle.

The projected DOS of Pd shows a small shift to lower energies after CO adsorption (0.60 eV). The computed IR frequencies for C–O adsorbed presents a red shift (compared with the gas phase CO) that agrees with experimental data reported in [9].

Acknowledgements

Our work was supported by ANPCyT through PICT 1770, and PIP-CONICET Nos. 114-200901-00272 and 114-200901-00068

research grants, as well as by SGCyT-UNS. A.J., E.A.G. and P.V.J. are members of CONICET. P.B. and S.A. are fellow researchers at this institution.

References

[1] A. Haghofer, K. Föttinger, F. Girgsdies, D. Teschner, A. Knop-Gericke, R. Schlögl, G. Rupprechter, J. Catal. 286 (2012) 13–21.
[2] N. Iwasa, T. Mayanagi, N. Ogawa, K. Sakata, N. Takezawa, Catal. Lett. 54 (3) (1998) 119–123.
[3] D.R. Palo, R.A. Dagle, J.D. Holladay, Chem. Rev. 107 (10) (2007) 3992–4021.
[4] N. Iwasa, T. Mayanagi, W. Nomura, M. Arai, N. Takezawa, Appl. Catal. A 248 (1) (2003) 153–160.
[5] N. Iwasa, N. Takezawa, Top. Catal. 22 (2003) 215–224.
[6] S. Penner, H. Lorenz, W. Jochum, M. Stöger-Pollach, D. Wang, C. Rameshan, B. Klötzer, Appl. Catal. A 358 (2009) 193–202.
[7] H. Lorenz, S. Penner, W. Jochum, C. Rameshan, B. Klötzer, Appl. Catal. A 358 (2009) 203–210.
[8] C. Rameshan, W. Stadlmayr, S. Penner, H. Lorenz, L. Mayr, M. Hävecker, R. Blume, T. Rocha, D. Teschner, A. Knop-Gericke, R. Schlögl, D. Zemlyanov, N. Memmela, B. Klötzer, J. Catal. 290 (2012) 126–137.
[9] K. Kovnir, M. Armbrüster, D. Teschner, T.V. Venkov, L. Szentmiklosi, F.C. Jentoft, A. Knop-Gericke, Y. Grin, R. Schlögl, Surf. Sci. 603 (10–12) (2009) 1784–1792.
[10] M. Armbrüster, K. Kovnir, D. Teschner, M. Behrens, Y. Grin, R. Schlögl, J. Am. Chem. Soc. 132 (2010) 14745–14747.
[11] A. Ota, M. Armbrüster, M. Behrens, D. Rosenthal, M. Friedrich, I. Kasatkin, F. Girgsdies, W. Zhang, R. Wagner, R. Schlögl, J. Phys. Chem. C 115 (2011) 1368–1374.
[12] M. Klanjšek, A. Gradišek, A. Kocjan, M. Bobnar, P. Jegli, M. Wencka, Z. Jaglicic, P. Popcevic, J. Ivkov, A. Smontara, P. Gille, M. Armbrüster, Y. Grin, J. Dolinšek, J. Phys.: Condens. Matter 24 (2012) 085703 (9p).
[13] S.E. Collins, M.A. Baltanas, A.L. Bonivardi, App. Catal. A: General 295 (2) (2005) 126–133.
[14] K. Kovnir, M. Armbrüster, D. Teschner, T.V. Venkov, F.C. Jentoft, A. Knop-Gericke, Y. Grin, R. Schlögl, Sci. Technol. Adv. Mater. 8 (5) (2007) 420–427.
[15] T. Skála, D. Baca, J. Libra, N. Tsud, V. Nehasil, S. Nemšák, K.C. Prince, V. Matolín, Thin Solid Films 517 (2008) 773–778.
[16] E. Hellner, F. Laves, Z. Naturforsch A2 (1947) 177–183.
[17] M.K. Bhargava, A.A. Gadalla, K. Schubert, J. Less-Comm. Met. 42 (1975) 69–76.
[18] G. Phragmen, Jernkontor. Ann. 107 (1923) 121.
[19] B.H. Verbeek, P.K. Larsen, W.M. Gerits, Vacuum 33 (1983) 813–814.
[20] M. Armbrüster, H. Borrmann, M. Wedel, Y. Prots, R. Giedigkeit, P. Gille, Z. Kristallogr, NCS 225 (2010) 617–618.
[21] G. Kresse, J. Hafner, Phys. Rev. B 47 (1993) 558–561.
[22] G. Kresse, J. Furthmüller, Phys. Rev. B 54 (1996) 11169–11186.
[23] G. Kresse, J. Furthmüller, Comput. Mater. Sci. 6 (1996) 15.
[24] D. Vanderbilt, Phys. Rev. B 41 (1990) 7892–7895.
[25] B. Hammer, L.B. Hansen, J.K. Nørskov, Phys. Rev. B 59 (1999) 7413–7421.
[26] H.J. Monkhorst, J.D. Pack, Phys. Rev. B 13 (1976) 5188–5192.
[27] R.F.W. Bader, Atoms in Molecules: A Quantum Theory, Oxford University Press, Oxford, 1990.
[28] G. Glockler, J. Phys. Chem. 62 (9) (1958) 1049–1054.
[29] R. Hoffmann, Solid & Surface. A Chemist's View of Bonding in Extended Structures, Wiley-VCH, New York, 1989.
[30] P. Ordejón, E. Artacho, J.M. Soler, Phys. Rev. B 53 (1996) R10441–R10444.
[31] J.M. Soler, E. Artacho, J.D. Gale, A. Garcia, J. Junquera, P. Ordejón, D. Sanchez-Portal, J. Phys. Condes. Matter 14 (2002) 2745–2779.
[32] P. Bechthold, P. Jasen, E. González, A. Juan, J. Phys. Chem. C 116 (2012) 17518–17524.
[33] R. Chen, Z. Chen, B. Ma, X. Hao, N. Kapur, J. Hyun, K. Cho, B. Shan, Theor. Chem. 987 (2012) 77–83.
[34] S. Pick, Surf. Sci. 603 (16) (2009) 2652–2657.
[35] L.O. Paz-Borbon, R.L. Johnston, G. Barcaro, A. Fortunelli, Eur. J. Phys. D 52 (2009) 131–134.
[36] N.R. Walker, J.K.-H. Hui, C.L. Gerry, J. Phys. Chem. A 106 (2002) 5803.
[37] M. Filatov, Chem. Phys. Let. 373 (2003) 131–135.
[38] Z.J. Wu, H.L. Li, H.J. Zhang, J. Meng, J. Phys. Chem. A 108 (2004) 10906–10910.
[39] V. Bertin, E. Agacino, R. López-Rendon, E. Poulain, J. Mol. Struct.: Teochem. 796 (2006) 243–248.
[40] N.Z. Schultz, B.F. Gherman, C.J. Cramer, D.G. Trohlar, J. Phys. Chem. B 110 (2006) 24030–24046.
[41] G. Zanti, D. Peeters, Eur. J. Inorg. Chem. 26 (2009) 3904–3911.
[42] B. Kalita, R.C. Deka, Eur. J. Phys. D 53 (2009) 51–58.
[43] M. Lischka, C. Mosch, A. Groß, Surf. Sci. 570 (2004) 227–236.
[44] G. Blyholder, J. Phys. Chem. 68 (1964) 2772–2777.
[45] A. Föhlisch, M. Nyberg, P. Bennich, L. Triguero, J. Hasselström, O. Karis, L.G.M. Pettersson, A. Nilsson, J. Chem. Phys. 112 (4) (2000) 1946–1959.
[46] A. Föhlisch, M. Nyberg, J. Hasselström, O. Karis, L.G.M. Pettersson, A. Nilsson, Phys. Rev. Lett. 85 (2000) 3309–3312.
[47] G. Herzberg, K.P. Huber, Molecular Spectra and Molecular Structure IV, Van Nostrand Reinhold Company, New York, 1979.